DEVELOPMENTAL DYNAMICS 241:1591–1602, 2012

Characterization and Functional Study of a Cluster of Four Highly Conserved Orphan Adhesion-GPCR in Mouse

Simone Prömel,[1,2]* Helen Waller-Evans,[1] John Dixon,[3] Dirk Zahn,[3] William H. Colledge,[4] Joanne Doran,[4] Mark B.L. Carlton,[3] Johannes Grosse,[3] Torsten Schöneberg,[2] Andreas P. Russ,[1] and Tobias Langenhan[1,5]*

Background: Adhesion G protein-coupled receptors (aGPCR) constitute a structurally and functionally diverse class of seven-transmembrane receptor proteins. Although for some of the members important roles in immunology, neurology, as well as developmental biology have been suggested, most receptors have been poorly characterized. Results: We have studied evolution, expression, and function of an entire receptor group containing four uncharacterized aGPCR: *Gpr110*, *Gpr111*, *Gpr115*, and *Gpr116*. We show that the genomic loci of these four receptors are clustered tightly together in mouse and human genomes and that this cluster likely derives from a single common ancestor gene. Using transcriptional profiling on wild-type and knockout/LacZ reporter knockin mice strains, we have obtained detailed expression maps that show ubiquitous expression of *Gpr116*, co-expression of *Gpr111* and *Gpr115* in developing skin, and expression of *Gpr110* in adult kidney. Loss of *Gpr110*, *Gpr111*, or *Gpr115* function did not result in detectable defects, indicating that genes of this aGPCR group might function redundantly. Conclusions: The aGPCR cluster *Gpr110*, *Gpr111*, *Gpr115*, and *Gpr116* developed from one common ancestor in vertebrates. Expression suggests a role in epithelia, and one can speculate about a possible redundant function of GPR111 and GPR115. *Developmental Dynamics 241:1591–1602, 2012.*

Key words: adhesion-GPCR; gene cluster; evolutionary conserved; epithelium

Key findings

- The cluster of four adhesion-GPCR *Gpr110*, *Gpr111*, *Gpr115*, and *Gpr116* is highly conserved in vertebrate evolution.
- *Gpr116* is expressed ubiquitously in mice tissue, *Gpr110* is strongly expressed in the renal pelvis.
- *Gpr111* and *Gpr115* are redundantly expressed in squamous epithelia in mice.
- *Gpr111* and *Gpr115* are expressed during embryonic development in the skin starting at embryonic day 12 with the formation of the basal layer of the skin.

Accepted 15 July 2012

[1]Department of Biochemistry, University of Oxford, Oxford, United Kingdom
[2]Institute of Biochemistry, Molecular Biochemistry, Medical Faculty, University of Leipzig, Leipzig, Germany
[3]Takeda Cambridge Ltd, Cambridge, United Kingdom
[4]Department of Physiology, Development and Neuroscience, University of Cambridge, Cambridge, United Kingdom
[5]Institute of Physiology, University of Würzburg, Würzburg, Germany
Grant sponsor: The Wellcome Trust; Grant number: WT075336/Z/04/A; Grant sponsor: BBSRC; Grant number: BB/C504200/1; Grant sponsor: Daimler-Benz Foundation; Grant number: 02-24/06; Grant sponsor: Deutsche Forschungsgemeinschaft; Grant number: La 2861/1-1; Grant sponsor: IZKF Würzburg; Grant number: Z-3/12.
***Correspondence to: Tobias Langenhan, Institute of Physiology, University of Würzburg, Röntgenring 9, 97070 Würzburg, Germany. E-mail: tobias.langenhan@uni-wuerzburg.de or Simone Prömel, Institute of Biochemistry, Molecular Biochemistry, University of Leipzig, 04103 Leipzig, Germany. E-mail: Simone.Proemel@medizin.uni-leipzig.de**

DOI 10.1002/dvdy.23841
Published online 4 September 2012 in Wiley Online Library (wileyonlinelibrary.com).

INTRODUCTION

Adhesion class G protein-coupled receptors (aGPCR) are seven-transmembrane (7TM) molecules that are exceptional in various aspects. From a phylogenetic perspective, they define the second largest class within the GPCR superfamily. Mammalian genomes possess 33 identified members clustered in nine groups (Bjarnadottir et al., 2004). aGPCR can already be distinguished in unicellular eukaryotes and primitive animals rendering them one of the oldest GPCR designs in evolution (Nordstrom et al., 2009).

The molecular architecture of aGPCR is unusual among the five GPCR classes in that they contain large ectodomains that contain a wide selection of protein domains, some of which have been found in adhesive contexts. The defining structural feature of all aGPCR is the GPCR proteolytic site (GPS) motif (Krasnoperov et al., 1997), a juxtamembrane sequence embedded within a larger GPCR-autoproteolysis-inducing (GAIN) domain (Arac et al., 2012), which promotes proteolytic cleavage of an aGPCR pro-receptor into a two-subunit heteromeric complex (Lin et al., 2004).

The functional contexts in which different aGPCR paralogs serve is very diverse, ranging from immunity, synapse function, planar cell polarity, tumor progression, and fertility (Usui et al., 1999; Steinert et al., 2002; Davies et al., 2004; Lin et al., 2005). Unraveling aGPCR function has not been possible for most class members due to the lack of knowledge about physiological stimuli and intracellular coupling to signaling cascades, and suitable in vivo models.

We have recently started a two-tiered approach to study aGPCR function using the invertebrate and vertebrate models *Caenorhabditis elegans* and mouse side-by-side. The nematode system allows rapid and highly scalable testing of molecular requirements for aGPCR function in vivo by means of transgenic introduction of receptor variants in an aGPCR null background. We have used this strategy to systematically uncover the requirement of conserved protein domains in the N terminus of the latrophilin-type aGPCR LAT-1 (Vakonakis et al., 2008; Langenhan et al., 2009). Using this approach, we have recently shown that cleavage at the GPS motif is not necessary for activity of LAT-1 in development and fertility, that the "split-personality" hypothesis, the ambiguous pairing of cleaved N- and C-terminal subunits of different aGPCR (Silva et al., 2009), is not required for LAT-1 function in the worm, and that two different signal activities are relayed through the LAT-1 receptor (Prömel et al., 2012). In addition to dissecting molecular dependencies of aGPCR signals, the worm also permits analysis of genetic interactions for the two invertebrate aGPCR groups, latrophilins and Flamingo/CELSR, under physiological conditions. Using the nematode toolkit, we implicated latrophilins in anterior–posterior tissue polarity in the nematode, a previously unknown property of latrophilins (Langenhan et al., 2009).

A complementary approach focuses on mammalian aGPCR to investigate their physiological repertoire using an established mouse transgenics pipeline to study the expression profile and loss-of-function effects of target aGPCR genes (Aparicio and Powell, 2004). This initiative has revealed that *Gpr126*, a vertebrate aGPCR essential for the myelination of peripheral nerves by Schwann cells (Monk et al., 2009, 2011), is required for embryonic viability and cardiovascular development in the mouse (Waller-Evans et al., 2010).

We have extended our analysis to vertebrate aGPCR genes with unclear or no functional affiliation. Here, we present our initial findings about a syntenic cluster of four loci, *Gpr110* (GenBank accession no. AY140952), *Gpr111* (GenBank accession no. AY140953), *Gpr115* (GenBank accession no. AY140957), and *Gpr116* (GenBank accession no. AY140958). They have been classified as novel aGPCR in human and encode putative aGPCR in the mouse genome (Fredriksson et al., 2002; Bjarnadottir et al., 2007; Haitina et al., 2008; Lum et al., 2010). *Gpr116* was initially named Ig-Hepta because of its two immunoglobulin and 7TM spanning domains (Abe et al., 1999). Furthermore, it was shown that the highly glycosylated Ig-Hepta exists as a disulphide-linked dimer, is expressed in rat lung and kidney, and is cleaved not only at the GPS motif but also at the SEA domain (Abe et al., 2002; Fukuzawa and Hirose, 2006). *Gpr110* was identified as a proto-oncogene in a retroviral insertion mutagenesis screen in the mouse and shows high expression levels in lung and prostate cancer suggesting a role in tumor pathology (Lum et al., 2010). In contrast, no information is available about *Gpr111* and *Gpr115*.

In this study, we characterize expression and explore the physiological context of four novel aGPCR of unknown function. Expression

Fig. 2. The four adhesion class G protein-coupled receptors (aGPCR) genes are highly conserved during vertebrate evolution. **A:** Schematic representation of the clustered aGPCR loci (blue and red) with syntenic genes (pale yellow) in different species (*Homo sapiens*/human, *Pan troglodytes*/chimpanzee, *Macaca mulatta*/macaque, *Nomascus leukogenys*/baboon, *Gorilla gorilla*/gorilla, *Pongo abelii*/oran utan, *Tarsius syrichta*/tarsier, *Microcebus murinus*/mouse lemur, *Tupaia belangeri*/tree shrew, *Mus musculus*/mouse, *Rattus norvegicus*/rat, *Felis catus*/cat, *Bos tauris*/cow, *Echinops telfarii*/tenrec, *Dasypus novemcinctus*/armadillo, *Monodelphis domestica*/opossum, *Pteropus vampyrus*/megabat, *Myotis lucifugus*/microbat, *Loxodonta africans*/elephant, *Ornithorhynchus anatinus*/platypus, *Tursiops truncates*/dolphin, *Gallus gallus*/chicken, *Taeniopygia guttata*/zebra finch, *Meleagris gallopavo*/turkey, *Xenopus tropicalis*/frog, *Anolis carolinensis*/anole lizard, *Danio rerio*/zebrafish, *Tetraodon negroviridis*/tetraodon, *Takifugu rubripes*/fugu, *Gasterosteus aculeatus*/stickleback, *Latimeria chalumnae*/coelacanth, *Gadus morhua*/cod, *Oryzias latipes*/medaka). Synteny and direction of the non-aGPCR genes is conserved throughout all species. From fish to primates, the number of GPCR genes increases. *Gpr111* and *Gpr115* are only present in land-living animals but are not a requirement for terrestrial life (e.g., lizard). Genomic sequences were taken from Ensembl21 and NCBI GenBank and analyzed to determine conserved regions. Where genes have not been properly annotated yet, gene names refer to homologs in primates and rodents. **B:** Phylogenetic tree based on cDNA sequence analysis of the seven-transmembrane (7TM) region of the clustered aGPCR. The phylogenetic tree was constructed using the PHYLIP (Phylogeny Interference Package; Felsenstein, 1989), version 3.5c (Felsenstein 1993, distributed by the author. Department of Genetics, University of Washington, Seattle) from SDSC Biology Workbench (Higgins et al., 1992; Thompson et al., 1994; Lim and Zhang, 1999) unrooted phylogenetic tree application of SDSC Biology WorkBench. Human CELSR1 was used as an outgroup.

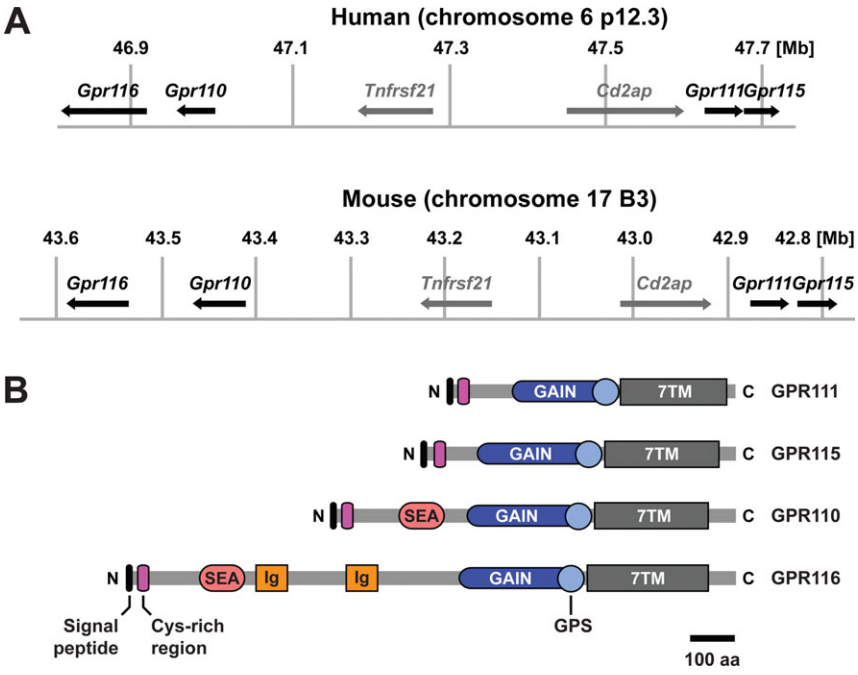

Fig. 1. Location and protein structure of adhesion class G protein-coupled receptors (aGPCR) *Gpr110*, *Gpr116*, *Gpr111*, and *Gpr115*. **A:** Gene cluster containing four uncharacterized aGPCR loci in human and mouse genomes. **B:** Primary domain structure prediction of the aGPCR. Note the presence of GAIN/GPS-7TM domain in all receptors. 7TM, seven-transmembrane domain; GAIN, G protein-coupled receptor autoproteolysis inducing domain; GPS, G protein-coupled receptor proteolytic site; Ig, immunoglobulin; SEA, sea urchin sperm protein/enterokinase/agrin.

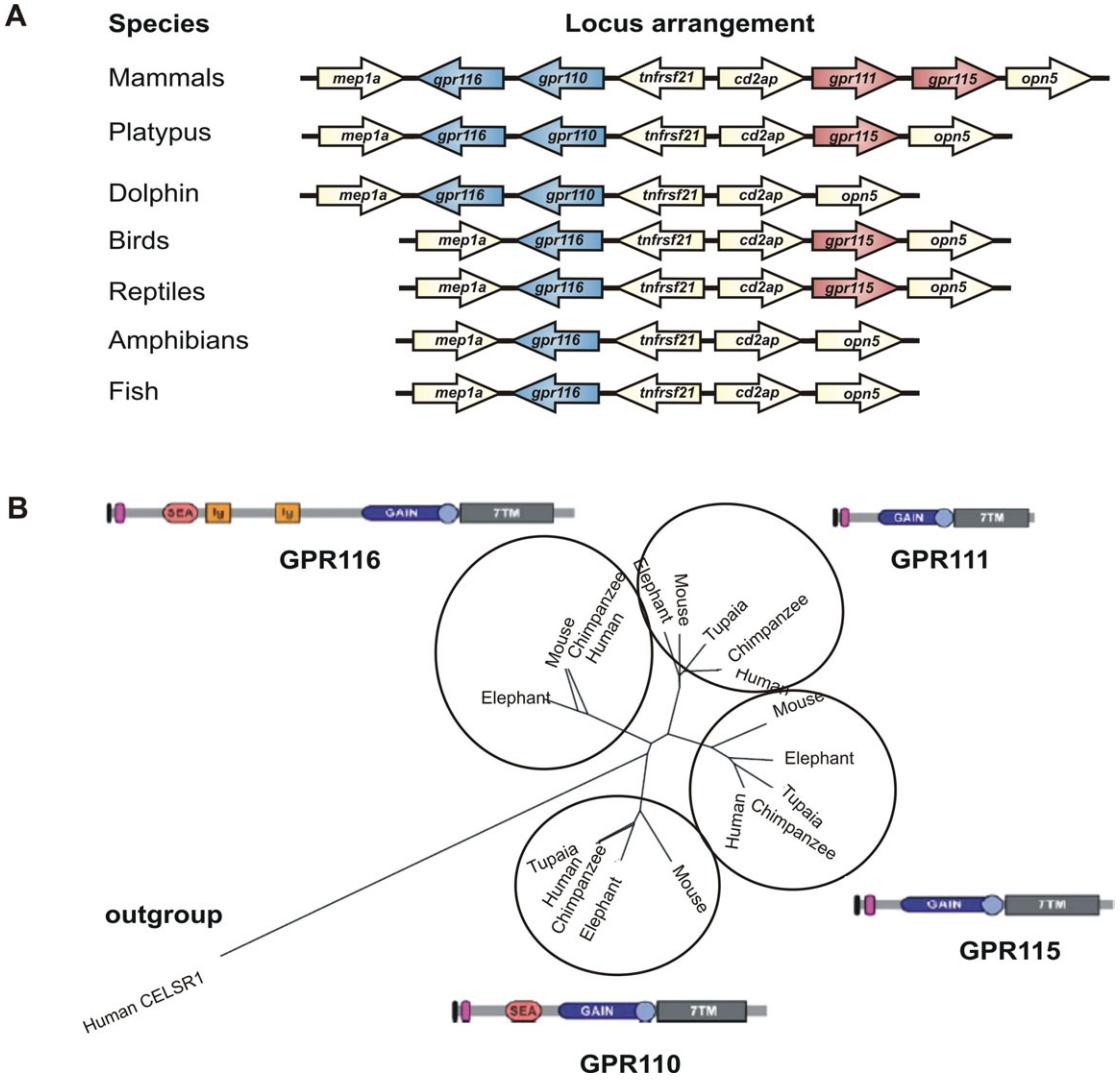

Fig. 2.

analysis and evolutionary studies reveal that the four receptor genes form a syntenic cluster and are as old as vertebrates, having potentially evolved from one common ancestor. *Gpr111* and *Gpr115*, only present in land living animals, show similar expression in squamous epithelia, indicating an overlapping function in these tissues.

RESULTS AND DISCUSSION

The aGPCR Cluster *Gpr110/111/115/116* Is Highly Conserved During the Evolution of Vertebrates

Previous phylogenetic analyses of the 7TM domain sequence of the entire human GPCR set distinguished five GPCR classes. According to the GRAFS nomenclature system, these classes were named Glutamate, Rhodopsin, Adhesion, Frizzled/Taste2, and Secretin (Fredriksson et al., 2003). Further subgrouping of the adhesion class based on their transmembrane regions and N-terminal domain sequences identified nine aGPCR groups (I–IX), which are present in mammalian genomes (Bjarnadottir et al., 2004).

aGPCR group VI encompasses five predicted aGPCR, *Gpr110*, *Gpr111*, *Gpr113*, *Gpr115*, and *Gpr116*. For subsequent gene targeting, we selected three group VI loci. Interestingly, all group VI aGPCR loci except for *Gpr113* are clustered within 0.9 Mb on chromosome 6p12.3 in human and on chromosome 17 in mouse genomes (Fig. 1A). At these locations, *Gpr111/Gpr115* and *Gpr110/Gpr116* are arranged in a tandem manner on the forward and reverse strand, respectively. Both aGPCR tandem configurations are present syntenically with a group of five non-aGPCR genes, in which the specific arrangement of all loci is preserved between mouse and human genomes (Fig. 1A).

We addressed the question of when during evolution the cluster was formed. To this end, we analyzed the genomic region harboring the *Gpr110/111/115/116* cluster from two invertebrates (*Caenorhabditis elegans*, *Drosophila melanogaster*) and 33 vertebrate species for the presence and structure of the clustered genes. This analysis was based on the syntenic relationship of all loci of the cluster containing also four non-GPCR genes (Fig. 2A) as well as on sequence analyses. No locus of the cluster could be found in invertebrate genomes. However, in all assayed vertebrate genomes, the cluster was conserved as apparent by order and direction of the non-aGPCR loci and the presence of at least one aGPCR gene. Identified aGPCR genes were confirmed by sequence analysis and comparison with the sequence of the respective human gene (Fig. 2A). Primates and all other mammals except for dolphin and platypus exhibit the complete cluster of all four receptor genes. While platypus possesses both genes of the tandem *Gpr110/Gpr116* but only one copy of the tandem *Gpr111/Gpr115*, presumably *Gpr115*, the dolphin genome only contains the tandem *Gpr110/Gpr116*.

In contrast, the gene clusters of birds and *X. tropicalis* contain one receptor gene of each tandem, *Gpr115* or *Gpr116* (Fig. 2A). Appearance of the *Gpr115* and *Gpr111* loci coincides with the evolution of land-living animals. All placental animals possess both loci of the tandem *Gpr110/Gpr116* independent of their adaptation to terrestrial life. Animals partially adapted to terrestrial life such as reptiles and birds possess only *Gpr115* and *Gpr116*. The second receptor of the tandem, *Gpr111*, is only present in land-living mammals. Analysis of aquatic vertebrates showed that the cluster is also evolutionarily conserved in fish. Fish display one gene of the tandem *Gpr110/Gpr116*, but neither *Gpr111* nor *Gpr115*. As the dolphin evolved from land-living animals, we speculate that it has lost the respective receptors of the tandem *Gpr111/Gpr115* after re-adaptation to aquatic life. The occurrence of only one aGPCR gene in the cluster very early in vertebrate evolution and the subsequent emergence of additional aGPCR loci in the cluster indicate that the receptors may have evolved from one common ancestor. The other half of the cluster (*Gpr115* and *Gpr111*) could have appeared by means of a gene inversion event which occurred independently in amphibians and birds or in the common ancestor of tetrapods and was lost in reptiles and birds as well as the dolphin after they split. Each half of the cluster might have undergone duplication resulting in the current cluster pattern that is detected in land-living mammals.

Alignment and analysis of cDNA sequences of the 7TM confirm that the receptor genes are more closely related to each other than to the loci of the other tandem (Fig. 2B). Primary amino acid sequence similarity analysis between each possible pair of aGPCR within the cluster supports this observation. The most similar receptor pairs are GPR116 and GPR110 with 32% similarity, and GPR111 and GPR115 with 65%. Additional sequence analyses revealed that none of the receptors displayed a SEA domain before the inversion event. The SEA domain can be detected in *Gpr116* of *X. tropicalis* for the first time during evolution, suggesting that the gene inversion happened before the development of the SEA domain (Figs. 1B, 2A). However, it cannot be excluded that the SEA domain was present in the common ancestor but was lost later in GPR111 and GPR115. By duplication, *Gpr110* might then have subsequently obtained a domain architecture similar to *Gpr116*, containing a SEA domain.

GPR111 and GPR115 Are Not Autoproteolyzed at the GPS Motif

Analysis of the longest splice variant and prediction of protein sequences of all four receptor genes revealed that they are composed of a large N terminus containing a signal peptide, a Cys-rich sequence, a GPS motif, and a 7TM domain displaying all structural properties of aGPCR (Fig. 1B). Additionally, *Gpr110* and *Gpr116* encode a SEA (sea urchin sperm protein/enterokinase/agrin) domain in their predicted ectodomains, and GPR116 exhibits two additional immunoglobulin-like domains as described for the rat ortholog (Abe et al., 1999).

The GPS motif is the central structural component of the aGPCR class of 7TM receptors. It is required for cleavage of aGPCR pro-receptor molecules and mediates noncovalent reassociation of the cleaved fragments (Arac et al., 2012). However, GPS

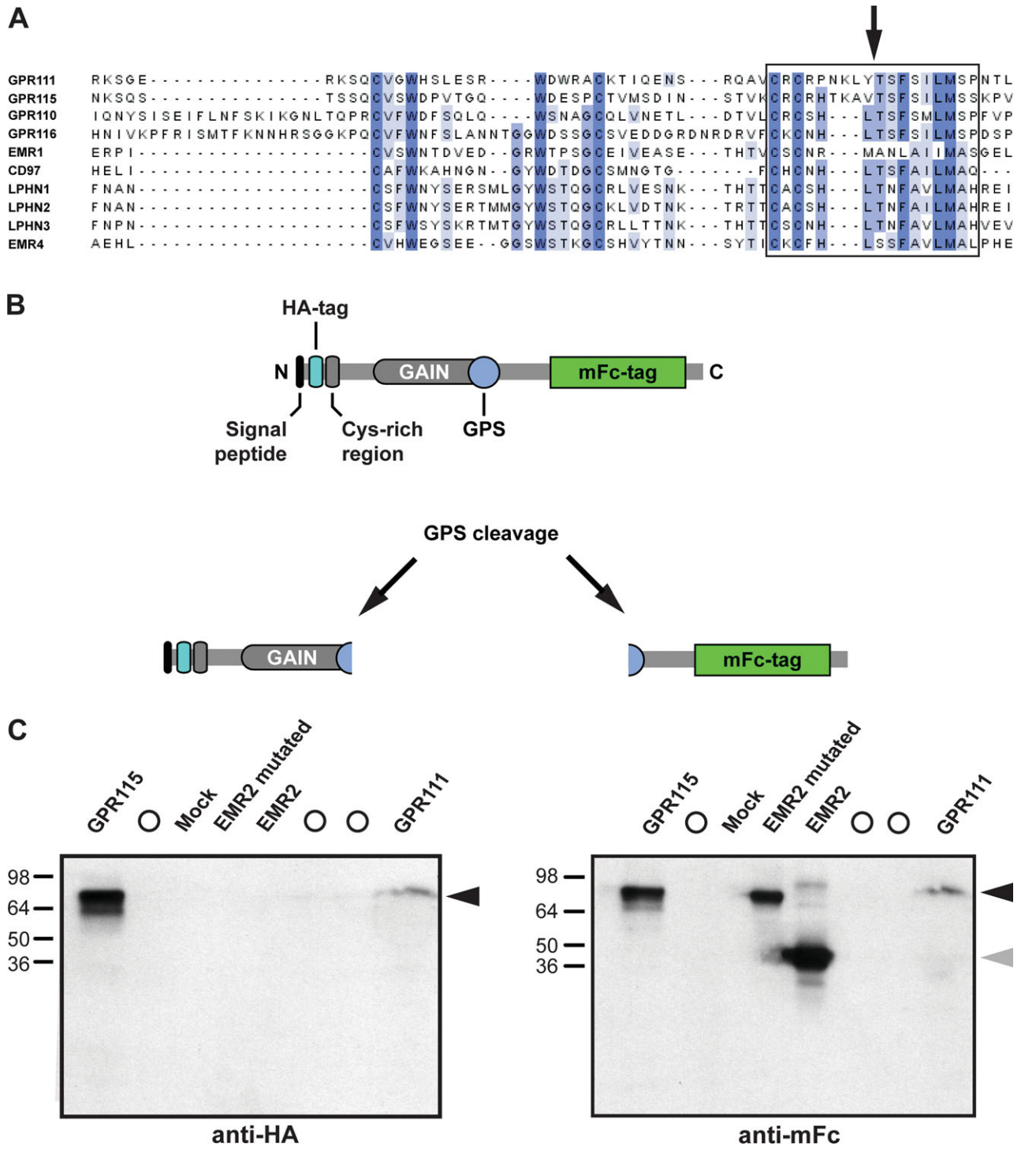

Fig. 3. GPR111 and GPR115 are not cleaved at the GPS motif. **A:** Alignment of mammalian adhesion class G protein-coupled receptors (aGPCR) homologs demonstrating that the GPS motif consensus sequence (boxed residues) is found in GPR110, GPR116, CD97, LPHN1/CIRL, and EMR4, but is altered in GPR111, GPR115, and EMR1 receptors. The site of GPS cleavage is indicated by an arrow. **B:** Construct design for GPS cleavage test of GPR111 and GPR115. **C:** Western blot results of conditioned medium detecting the N-terminal HA-tag (left panel) and the C-terminal mFc-tag of GPR111 and GPR115 (right panel). Both receptors are GPS cleavage-deficient and are found as a full-length protein in the medium (black arrowhead). GPS cleavage-competent EMR2 receptor control shows the generation of noncleaved (black arrowhead) and cleaved (gray arrowhead) fragments, while a GPS-deficient EMR2 mutant is found in full-length only. Note that these transgenes are not HA-tagged and are therefore invisible on the HA-probed blot. Open circles represent lanes that were not loaded with protein.

cleavage is dispensable for aGPCR function and the consensus GPS sequence is frequently lost in individual aGPCR homologs (Prömel et al., 2012). Thus, the physiological relevance of GPS cleavage and the functional difference between cleavable versus noncleavable aGPCR have remained controversial to date.

Our results on the evolutionary history of the *Gpr110/111/115/116* aGPCR cluster revealed an interesting variation in the GPS sequence of the *Gpr111/Gpr115* receptor tandem. While GPR110 and GPR116 exhibit the consensus GPS sequence, in GPR111 and GPR115 the sequence is altered (Fig. 3A). Both are lacking a conserved leucine and have a three amino acid insertion between the site of this leucine and an N-terminal histidine essential for cleavage in other aGPCR (Lin et al., 2004). GPR111 is also lacking this histidine (Fig. 3A). Both modifications would be predicted to result in noncleavage at the GPS motif.

To directly assay cleavage in these receptors, we expressed GPR111 and GPR115 constructs with an N-terminal HA-tag and a C-terminal mFc-tag in HEK293 cells and analyzed conditioned medium using conventional Western blotting with specific antibodies against both tags (Fig. 3B). GPS cleavage would generate two separate protein bands (cleaved and noncleaved) that would be detected by both antibodies, whereas cleavage-deficiency results in a single noncleavaged protein fraction. As controls, we used a similar EMR2 construct (Lin et al., 2004), a mammalian aGPCR known to undergo GPS proteolysis, and a GPS-mutated EMR2 variant which is resistant to autoproteolytic cleavage (Chang et al., 2003). Both control transgenes were only C-terminally mFc-tagged but did not contain an N-terminal HA-tag.

As expected, cleavage-competent EMR2 was detected on Western blots as noncleaved and cleaved fragments, while cleavage-deficient EMR2 resulted in a single band at the expected size of 80 kDa (Fig. 3C). Using both antisera, GPR111 and GPR115 exhibited a similar pattern on Western blots with only one large protein band corresponding in size to the full-length, noncleaved receptors (Fig. 3C). We conclude that GPR111 and GPR115 are not autoproteolyzed at the GPS motif due to loss of the consensus cleavage site, rendering them another instance of aGPCR in mammals where GPS-cleavage deficiency has been directly shown (M. Stacey, personal communication).

Generation of *Gpr110*, *Gpr111*, and *Gpr115* Knockout/LacZ Reporter Knockin Alleles

To investigate the function and expression of this aGPCR cluster in vivo, we generated knock-out/LacZ knock-in mouse strains for three uncharacterized receptor genes: *Gpr110*, *Gpr111*, and *Gpr115*. For each receptor, targeted mutations disrupting the coding regions were introduced in murine embryonic stem cells. A part of the 7TM, including the entire first transmembrane span, was replaced with a neomycin resistance cassette and a *lacZ* (β-*Gal*) expression marker to follow the expression pattern of the genes in detail (Fig. 4A).

Homologous recombination to the correct genomic locus was verified with conventional Southern blotting and polymerase chain reaction (PCR) genotyping for each targeted mouse strain (Fig. 4B,C).

Loss-of-Function of *Gpr110*, *Gpr111*, and *Gpr115* Does Not Affect Development or Fertility

Gpr110, *Gpr111*, and *Gpr115* knockout/knockin mice were maintained on an inbred 129S6/SvEv genetic background. Phenotypic characterization of the strains revealed that their viability and fertility is indistinguishable from wild-type controls. To test fertility, mutant lines were bred as homozygous ($GprX^{LacZ}/GprX^{LacZ}$) and heterozygous ($GprX^{LacZ}/+$) pairs, and the numbers of offspring in each litter from these matings were compared (Fig. 5A). Litter sizes were indistinguishable between homozygous and heterozygous matings. The genotypes of offspring from heterozygous parents were determined by PCR genotyping and were present at Mendelian frequencies in each mutant line (Fig. 5B), indicating that no partially penetrant developmental phenotypes such as detrimental dominant activity result from removal of *Gpr110*, *Gpr111*, or *Gpr115* function. Each mutant strain was also backcrossed five times to C57Bl/6 and MF1 strains respectively, and no background-specific phenotypes were observed. However, a more detailed characterization could reveal more subtle phenotypes and is currently in process.

Gpr116 Is Ubiquitously Expressed and *Gpr110* Is Expressed in Kidney

To obtain transcriptional expression profiles of all four clustered aGPCR, we performed reverse transcriptase PCR (RT-PCR) analysis on tissues of adult mice. The results revealed distinct expression patterns for each of the four receptors (Fig. 6).

Previous transcriptional profiling indicated that *Gpr116* is expressed in lung, placenta, heart, and eyecup, whereas *Gpr110* transcript was found in cornea, liver, and ciliary bodies (Wu et al., 2009).

We found that *Gpr116* is ubiquitously expressed (Fig. 6; Abe et al., 1999). *Gpr110*, which is in a tandem with *Gpr116*, is more distinctly expressed in liver, kidney, and adrenal gland (Fig. 6). Strong expression of *Gpr110* in the kidney of mice is consistent with previous results observed in human samples (Lum et al., 2010). To confirm receptor expression within these tissues, $Gpr110^{LacZ/LacZ}$ mice were stained with X-Gal. Kidneys of $Gpr110^{LacZ/LacZ}$ mice exhibited strong *LacZ* expression in the renal pelvis (Fig. 7) and the ureter, suggesting that *Gpr110* is present in urothelium. *Gpr110* expression in the liver could not be corroborated by *LacZ* expression analysis, likely due to low *LacZ* expression levels and endogenous hepatic β-galactosidase activity, resulting in varying *LacZ* background staining.

Gpr111 and *Gpr115* Are Expressed in Squamous Epithelia

Strong overlapping expression of *Gpr111* and *Gpr115* was detected in the skin, and more weakly in lung, heart and kidney (Fig. 6). *Gpr111* was mainly expressed in skin and heart, and very weakly in lung and spleen, which is consistent with large-scale microarray datasets (Wu et al., 2009). To corroborate receptor expression within these tissues, $Gpr111^{LacZ/LacZ}$ mice were stained with X-Gal. Strong *LacZ* expression was detected in all epidermal layers of skin (Fig. 8A

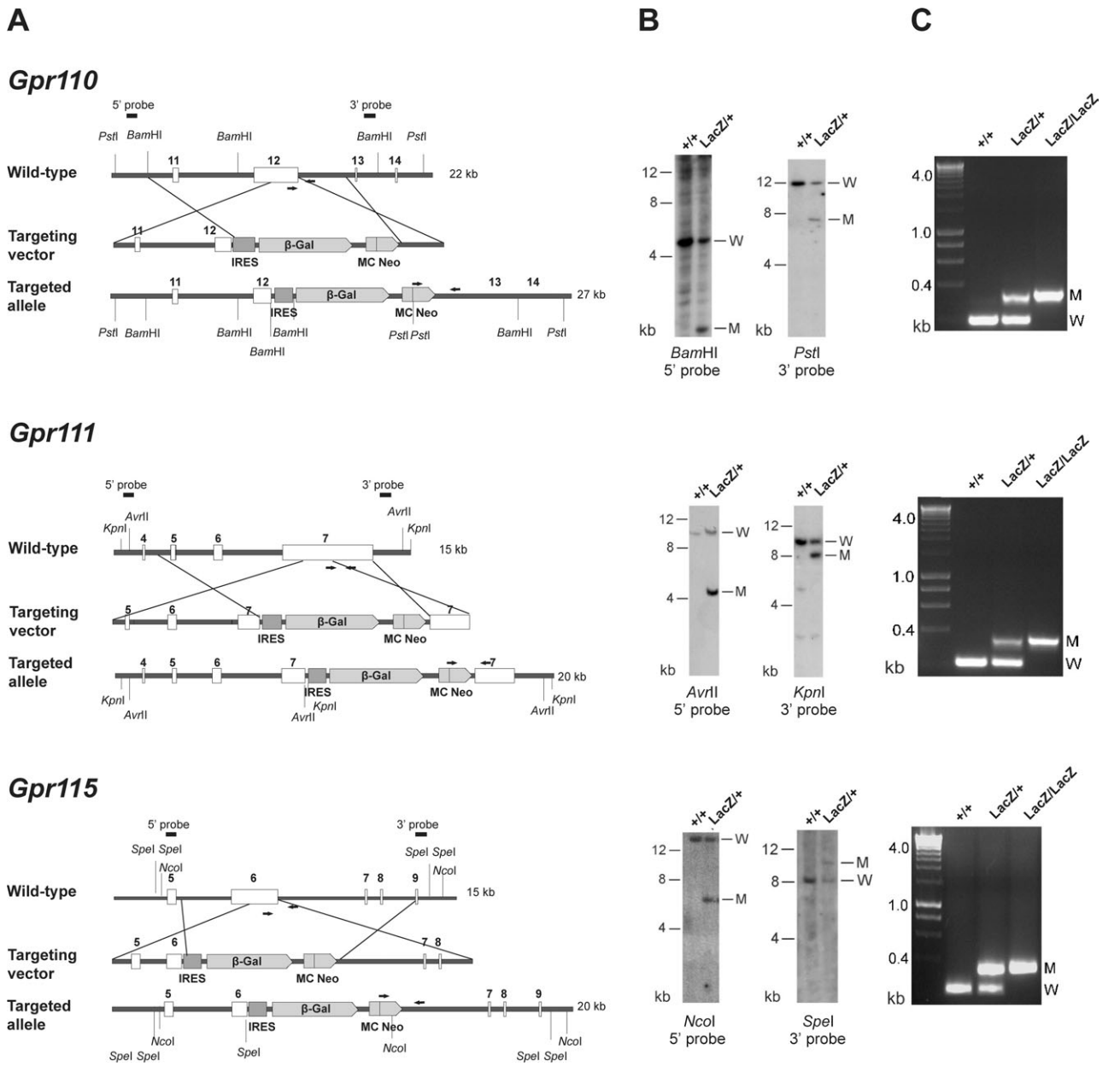

Fig. 4. Targeted disruption of mouse *Gpr110*, *Gpr111*, and *Gpr115* loci by homologous recombination. **A:** Schematic representations of the *Gpr110*, *Gpr111*, and *Gpr115* loci, targeting constructs and expected mutant alleles are shown. Probe positions for Southern blot analysis are indicated. IRES, internal ribosomal entry site; β-Gal, beta-galactosidase gene; MC, MC promoter; Neo, neomycin resistance gene. Thin arrows represent polymerase chain reaction (PCR) primers for genotyping of targeted mice. **B:** Southern analysis of *Gpr110*, *Gpr111*, and *Gpr115* targeted mice. Digested genomic DNA from mice wild-type or heterozygous for each targeted gene were hybridized with 5′ probes and 3′ probe shown in A. Hybridized fragments of wild-type (W) and mutant (M) alleles are shown. Enzymes used for digestion are shown below each panel. **C:** PCR-based genotyping of offspring from heterozygous *Gpr110*, *Gpr111*, and *Gpr115* matings demonstrating correct targeting. M, mutant band; W, wild-type band.

I–IV). This expression was observed in the developing skin at embryonic day (E) 14, but not at E11 (Fig. 8B). In mice, the epithelium of the skin starts to develop at E12 with the formation of the basal layer (Blanpain and Fuchs, 2006). Because *LacZ* expression may be delayed compared with the receptor gene, transcriptional expression of *Gpr111* in the developing skin was re-analyzed by RT-PCR. Transcripts were detected at E12, although at lower levels than at E16 and matches with the start of epidermis development (Fig. 8C). These results confirm LacZ expression data of *Gpr111*.

We analyzed other organs with stratified squamous epithelia for *Gpr111* expression and found $Gpr111^{LacZ}$ expression in the superficial epidermal layers of esophagus and tongue (Fig. 8A V–VIII, IX–XII). To investigate whether *Gpr111* expression is confined to squamous epithelia, we investigated the squamocolumnar junction in the mouse stomach located between the forestomach and stomach. At this junction, stratified squamous epithelial histoarchitecture transits to a monolayered columnar epithelium. Of interest, $Gpr111^{LacZ}$ expression is restricted to the stratified domain at

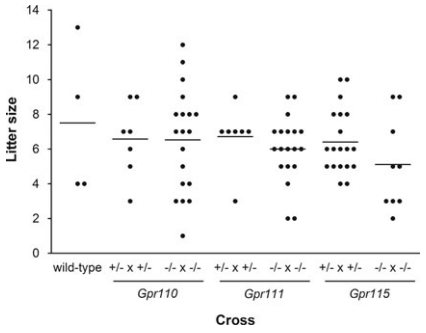

Fig. 5. Litter size and genotype distribution of *Gpr110*, *Gpr111*, and *Gpr115* knockout mice. **A:** Average litter sizes from −/− × −/− crosses and from ± × ± crosses. Average number of offsprings are shown with number of analyzed litters in parentheses. Unpaired *t*-test did not reveal any significant differences in litter size between crosses ($P > 0.05$). **B:** Distribution of genotypes among offspring from ± × ± crosses (n(*Gpr110*) = 38, n(*Gpr111*) = 40, n(*Gpr115*) = 112). χ^2 tests did not show any significant difference from a 1:2:1 ratio ($P > 0.05$).

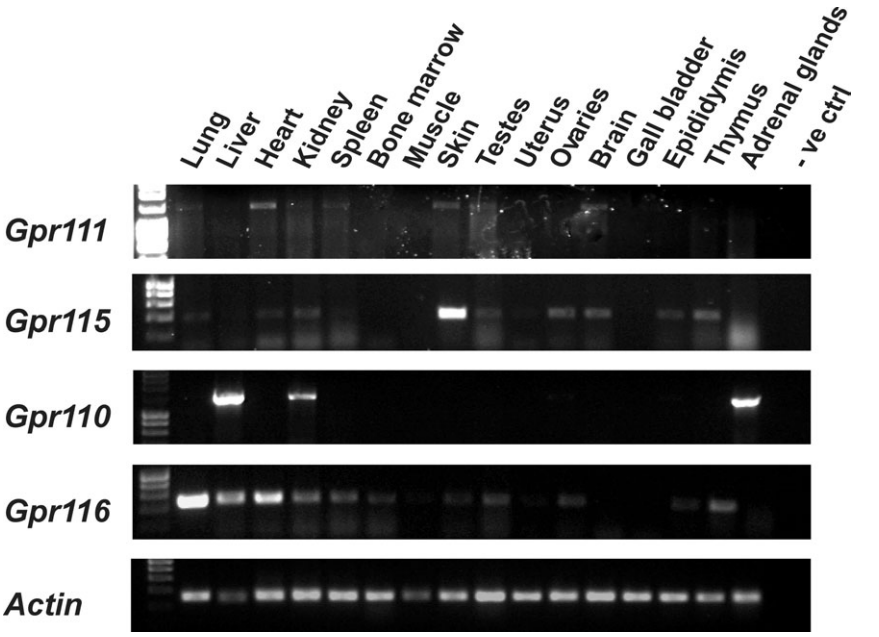

Fig. 6. Organ-specific expression of adhesion class G protein-coupled receptors (aGPCR) tandems *Gpr111/Gpr115* and *Gpr110/Gpr116*. Reverse transcriptase polymerase chain reaction (RT-PCR) analysis of mRNA expression in different mouse tissues. Total RNA isolated from adult mouse tissues was transcribed into cDNA and assayed with receptor gene specific primers. Equal quantities of cDNA per reaction were confirmed by PCR with actin-specific primers. Note that expression of tandem partners only partially overlaps indicating differential transcriptional regulation of the receptors.

the squamocolumnar junction, suggesting that *Gpr111* expression is specific to this type of epithelium (Fig. 8A, XIII–XVI).

Based on the strong developmental expression of *Gpr111* in skin, we next tested whether *Gpr111* is required for formation of the skin barrier by a skin permeability assay using toluidine blue (Fig. 8D). Penetration of the dye is permitted as long as skin barrier formation is not completed yet, and thus staining of skin inversely correlates with barrier maturation. Full staining can be observed in barrierless embryos before E16, and no staining in embryos with fully intact skin barrier after E17 (Hardman et al., 1998). In $Gpr111^{LacZ/LacZ}$ mice, skin barrier formation starts at E16 and continues at the same rate and pattern as in control animals (Fig. 8D). Hence, formation of the skin barrier in $Gpr111^{LacZ/LacZ}$ mice appears normal.

Gpr115, which is in a tandem with *Gpr111*, was highly expressed in a similar tissue profile as *Gpr111* as shown by RT-PCR (Fig. 6). In addition, *Gpr115* transcript could also be weakly detected in testis, kidney, ovary, epididymis, and thymus (Fig. 6). Similarly to *Gpr111*, the onset of *Gpr115* expression coincides with the development of the skin in embryos. Unfortunately, X-Gal staining of organs from $Gpr115^{LacZ/LacZ}$ was precluded by a defective *LacZ* transcript.

Many significant changes in the skin appeared during adaptation of animals to the land. Formation of a corneous cell envelope, absent in fish, is characteristic for development of land-living animals (Alibardi, 2003). Both receptors of the *Gpr111/115* tandem are primarily expressed in the skin and only appear at a stage during evolution where adaptation of animals to the land started. Thus, a role of both aGPCR in skin specialization for terrestrial life can be hypothesized. Due to comparable expression patterns of *Gpr111* and *Gpr115* but lack of an overt phenotype in $Gpr111^{LacZ/LacZ}$ and $Gpr115^{LacZ/LacZ}$ individuals, it can be speculated that both receptors have potentially redundant functions in squamous epithelia. To test this hypothesis in future investigations, removal of both receptor functions would be required to uncover loss-of-function effects. Subsequent studies will also provide the opportunity to screen for more subtle defects in single and double mutant combinations of the receptor genes analyzed for the first time here.

Fig. 8. Organ-specific expression of *Gpr111* and *Gpr115*. **A:** PAS and X-Gal staining for LacZ expression in skin, esophagus, tongue, and stomach on paraffin sections of $Gpr111^{LacZ/LacZ}$ and wild-type mice. Expression is observed in all layers of epithelium above the basal membrane (dotted line in II, VI, X) in all three tissues. Scale bars = 100 μm, Scale bars XIII, XV = 1 mm. oe, esophagus; fs, forestomach; st, stomach. **B:** Developmental analysis of $Gpr111^{LacZ}$ expression in embryos demonstrates strong expression in the skin at embryonic day (E) 14. $Gpr111^{LacZ}$ expression in the epidermis of E14 embryos was also analyzed in paraffin sections showing restriction to the epidermal layers of the skin. Scale bars = 1 mm (embryo panels) and 100 μm (sections). **C:** Expression analysis of *Gpr111* and *Gpr115* in embryos by reverse transcriptase polymerase chain reaction (RT-PCR) confirms that both receptor genes are transcribed in the developing skin. **D:** Skin barrier development in $Gpr111^{-/-}$ embryos was visualized with toluidine blue staining. No difference could be observed between $Gpr111^{-/-}$ (top panel) and wild-type (bottom panel) mouse embryos ($Gpr111^{-/-}$: n = 7; wild-type: n = 9). Scale bars = 1 mm.

Developmental Dynamics

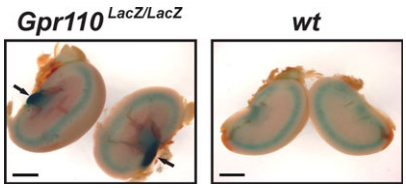

Fig. 7. *Gpr110* is expressed in the kidney. Expression of *Gpr110* in adult kidney of *Gpr110*$^{LacZ/LacZ}$ and a wild-type control. Strong expression was detected in the ureter (left panel, arrows). Note that staining in the renal medulla is also present in control animals lacking a *LacZ* cassette and, therefore, regarded unspecific. Kidneys were cut after staining. Scale bars = 2 mm.

Fig. 7.

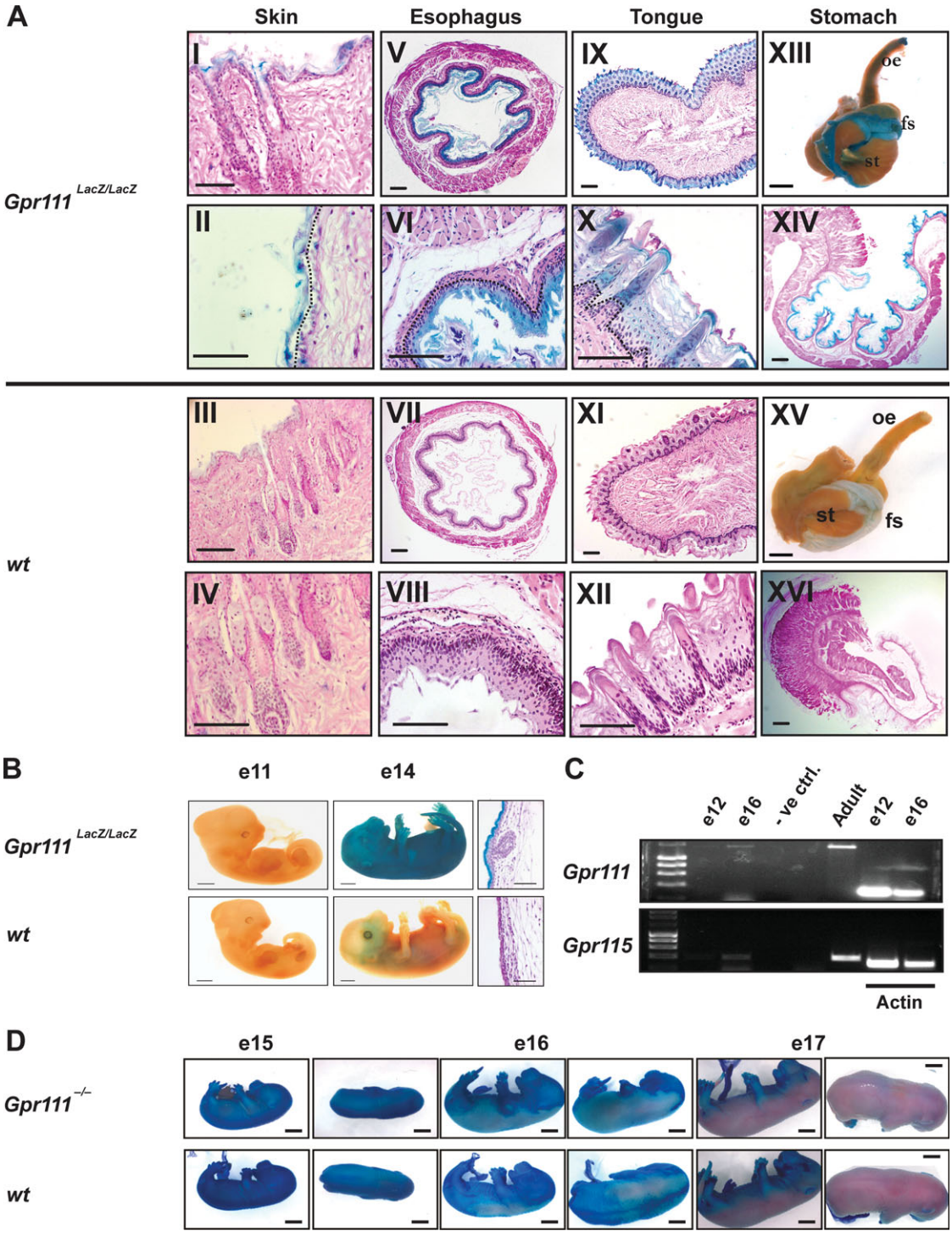

Fig. 8.

EXPERIMENTAL PROCEDURES

Ethics Statement

All procedures were carried out in accordance with the Animals (Scientific Procedures) Act 1986 and with the approval of local ethical review committees under the UK Home Office Project License PPL 30/2462.

Comparative Genomic Analysis

Genomic loci and predicted gene products for the GPR genes were obtained from the Ensembl database (http://www.ensembl.org) as well as from NCBI GenBank (http://www.ncbi.nlm.nih.gov/genbank/) and analyzed with the Geneious software package (Biomatters Ltd., Auckland, NZ) and NCBI BLAST (http://blast.ncbi.nlm.nih.gov/). Phylogenetic tree construction was conducted using the algorithms and PHYLIP (Phylogeny Interference Package; Felsenstein, 1989), version 3.5c (Felsenstein 1993, distributed by the author. Department of Genetics, University of Washington, Seattle) from SDSC Biology Workbench (Higgins et al., 1992; Thompson et al., 1994; Lim and Zhang, 1999).

Generation of Constructs

Fragments of *Gpr115* (amino acids 19–400) and *Gpr111* (amino acids 18–378) were amplified from murine cDNA with primers 5′-CCCAAGCTTGTACC CATACGATGTTCCAGATTACGCTGA TATCTGTAGGATATTATG CCAGGCC TCCAGCAAA-3′ and 5′-TAGTAGCGC GGCCGCCCTGCTTTCCAACGTGTT GGGAGAC ATTAGAAT-3′ for Gpr111 and 5′-CCCAAGCTTGTACCCATACG ATGTTCCAGATTACGCTG ATATCTC TCATTCCAAACCCAAGACTCACAGA AAA-3′ and 5′-TAGTAGCGCGGCCGC CCTTAC AGGCTTAGAAGACATGAG GATGGAGAA-3′ for *Gpr115*. The forward primers introduce an hemagglutinin (HA) tag to fuse to the cDNA and a *Hin*dIII site 5′ of the tag. The reverse primer introduced a *Not*I site. The PCR product was cut with *Hin*dIII and *Not*I, purified and ligated into a modified vector pSecTag2A containing an mFc tag with a stop codon upstream of the myc epitope (kind gift from Dr. M. Stacey, University of Leeds), which was also cut with *Hin*dIII and *Not*I. Constructs were transformed into chemically competent *E. coli* TOP10 cells (Invitrogen). Bacteria were grown at 37°C on LB agar plates with ampicillin.

Transfections

A total of 24 hr before transfection, 2.5×10^6 HEK293T cells were seeded in 6-cm dishes with 4 ml of DMEM (Gibco). Cells were transfected using calcium phosphate precipitation: 15 μg DNA were mixed with 25 mM $CaCl_2$, in a total volume of 500 μl. The 500 μl of 2× HBS (50 mM HEPES pH 7.05, 10 mM KCl, 12 mM dextrose, 280 mM NaCl, 1.5 mM Na_2HPO_4) were added, and then cells incubated in this solution. After 8 hr, the medium was discarded and 4 ml of CD293 Medium (Invitrogen) were added.

Protein Preparation and Western Blot Analysis

Conditioned medium was collected from cells 86 hr post transfection, pelleted by centrifugation, filtered through a 0.45-μm filter, and protease inhibitor (MiniComplete, Roche) was added. Protein was concentrated by methanol/chloroform precipitation as described previously (Wessel and Flugge, 1984) and resuspended in 2× Laemmli buffer.

Protein was subject to electrophoresis as described previously (Laemmli, 1970) in a 12.5% sodium dodecyl sulfate-polyacrylamide gel electrophoresis (SDS-PAGE) gel and transferred to a polyvinylidene difluoride membranes. Blots were then probed with the antibody goat anti-mouse IgG (Sigma) 1:10,000 or rat anti-HA high affinity (Roche) 1:10,000, respectively, overnight at 4°C. After washing, membranes were incubated for 1 hr at room temperature with horseradish-peroxidase–conjugated goat anti-rat (Jackson ImmunoResearch) or horseradish-peroxidase–conjugated horse anti-mouse (Vector) 1:10,000. Western blots were developed by an enhanced chemiluminescence (ECL) detection system (Amersham). For detection of actin as loading control, membranes were stripped in Stripping buffer (1% SDS, 0.1 M Tris pH 6.8, 0.175% β-mercaptoethanol) for 30 min at 50°C, blocked and probed with mouse anti-actin (Chemicon) 1:10,000, and then incubated with horseradish-peroxidase–conjugated horse anti-mouse (Vector) 1:10,000 as described above.

5-Bromo-4-chloro-3-indolyl β-D-galactoside (X-Gal) Staining

LacZ activity was detected by staining tissues with X-Gal. Mice were killed by cervical dislocation, tissues extracted, rinsed in PBS with 2 mM $MgCl_2$, and prefixed 40 min in 0.2% glutaraldehyde at 4°C. After washed with 100 mM $NaHPO_4$ (pH 7.4) plus 1 mM $MgCl_2$, 0.02% NP-40 and 0.01% $C_{24}H_{39}NaO_4$, X-Gal staining was performed overnight at 37°C in 100 mM $NaHPO_4$ (pH 7.4) plus 1.6 mg/ml X-Gal, 5 mM $K_3Fe(CN)_6$, 5 mM $K_4Fe(CN)_6$, 1 mM $MgCl_2$, 0.02% NP-40 and 0.01% $C_{24}H_{39}NaO_4$. Tissues were rinsed and post-fixed in 4% paraformaldehyde at 4°C.

Histology

X-Gal stained and post-fixed tissues were embedded in paraffin and sectioned at 10 μm thickness. Sections were rehydrated and stained by periodic-acid–Schiff reaction.

Microscopy

Whole-mount specimens were photographed using a Nikon SMZ1500 dissection microscope fitted with a Leica DC500 camera. Histological sections were documented using a Zeiss Axioplan2.0 microscope fitted with an AxioCam HD camera. Images were modified using Adobe Photoshop 9.0.

RT-PCR

Mice were killed by cervical dislocation, tissues removed, ground, and incubated in TRIzol reagent (Invitrogen, Paisley, UK) for total RNA isolation according to manufacturer's protocol. cDNA was obtained with a reverse transcriptase (RT) and random hexamer primers. Samples were also subject to the same conditions without addition of reverse transcriptase enzyme as controls for potential DNA contamination of the transcribed cDNA library. To detect the

expression of the receptor transcripts, the following PCR primers were used. *Gpr110*: forward 5′-GGCATCCAGTCC ACGAGTAT-3′ and reverse 5′-ATGGA GAAAGAGGTCAGGTGA-3′; *Gpr116*: forward 5′-GAACAAGTCATACAGAA CCT-3′ and reverse 5′-TTCCATTCAA TACTGCTCCA-3′; *Gpr111*: forward 5′-CTTACACAACATCTCAACAA-3′ and reverse 5′-TGAGTAAGGAGAAG ATAATGTGGA-3′; *Gpr115*: forward 5′-TTCTCATTCCAAACCCAAGAC-3′ and reverse 5′-AACAATGCAAACGT AGTCCT-3′. All primers were designed to span either exon–exon boundaries or to bind in different exons. The housekeeping gene actin served as internal loading control. The PCR was performed as according to the following: 94°C for 2 min, followed by 28 cycles: 94°C for 30 s, 55°C for 40 s, 72°C for 2 min.

Generation of Gpr110, Gpr111, and Gpr115 Knockout Mice

Transgenic mice were maintained as an inbred stock on a 129S6/SvEv genetic background. The genomic sequences of the mouse *Gpr110*, *Gpr111*, and *Gpr115* genes were obtained from www.ensembl.org (transcript IDs: ENSMUSG 00000041293, ENSG00000164393, ENSG00000153294). The 5′ and 3′ flanking arms were amplified using genomic DNA from 129Sv/Ev mice. The vector for homologous recombination was constructed as described previously (Russ et al., 2000; Cash et al., 2008). Briefly, targeting constructs were created by inserting 5′ arms upstream of the *lacZ-Neo* cassette, and 3′ arms between the *lacZ-Neo* cassette and a thymidine kinase gene. The targeting constructs were linearized and electroporated into CCB embryonic stem cells derived from 129Sv/Ev mice. G418-resistant colonies were selected and expanded. Clones with homologous recombination were detected by Southern blot analysis using probes flanking the 5′ and 3′ arms and confirmed by PCR. Clones with the correct recombination event were obtained and injected into 129Sv/Ev mouse blastocysts. Chimeric males were bred with wild-type females and offspring tested for the presence of disrupted alleles by PCR using genomic ear DNA. Heterozygous mice were further bred to obtain homozygous *Gpr110*, *Gpr111*, and *Gpr115* KO mice. For mixed-background experiments, homozygous *Gpr110*, *Gpr111*, and *Gpr115* KO mice were crossed five times with MF1 mice and five times with C57Bl/6 mice. All experiments were performed under the authority of a U.K. Home Office Project License and were approved by a local ethics panel.

Presentation of Data and Statistical Analyses

Quantitative data were presented as raw values with means. Statistical comparisons were accomplished by unpaired *t*-test (equal variances) and χ^2. P values < 0.05 were considered statistically significant.

ACKNOWLEDGMENTS

S.P. was funded by studentships from the Daimler-Benz Foundation, and T.L. was funded by the Wellcome Trust, the Deutsche Forschungsgemeinschaft, the IZKF Würzburg, and Magdalen College, Oxford. Author contributions: S.P., H. W-E., and T.L. performed experiments; A.P.R. conceived the project; S.P., A.P.R., and T.L. wrote the manuscript. A.P.R. is a founder of Paradigm Therapeutics Ltd., which was acquired by Takeda Cambridge Ltd. This did not influence study design, data collection and analysis, decision to publish, or preparation of the manuscript. The mutant mouse strains for *Gpr110*, *Gpr111*, and *Gpr115* were generated by Takeda Cambridge Ltd. and made available for analysis under a material transfer agreement for academic research. The funders had no role in study design, data collection and analysis, decision to publish, or preparation of the manuscript.

REFERENCES

Abe J, Suzuki H, Notoya M, Yamamoto T, Hirose S. 1999. Ig-hepta, a novel member of the G protein-coupled hepta-helical receptor (GPCR) family that has immunoglobulin-like repeats in a long N-terminal extracellular domain and defines a new subfamily of GPCR. J Biol Chem 274:19957–19964.

Abe J, Fukuzawa T, Hirose S. 2002. Cleavage of Ig-Hepta at a "SEA" module and at a conserved G protein-coupled receptor proteolytic site. J Biol Chem 277:23391–23398.

Alibardi L. 2003. Adaptation to the land: the skin of reptiles in comparison to that of amphibians and endotherm amniotes. J Exp Zool B Mol Dev Evol 298:12–41.

Aparicio SA, Powell J. 2004. Genetic approaches to unraveling G protein-coupled receptor biology. Curr Opin Drug Discov Devel 7:658–664.

Arac D, Boucard AA, Bolliger MF, Nguyen J, Soltis SM, Sudhof TC, Brunger AT. 2012. A novel evolutionarily conserved domain of cell-adhesion GPCR mediates autoproteolysis. EMBO J 31:1364–1378.

Bjarnadottir TK, Fredriksson R, Hoglund PJ, Gloriam DE, Lagerstrom MC, Schioth HB. 2004. The human and mouse repertoire of the adhesion family of G-protein-coupled receptors. Genomics 84:23–33.

Bjarnadottir TK, Geirardsdottir K, Ingemansson M, Mirza MA, Fredriksson R, Schioth HB. 2007. Identification of novel splice variants of Adhesion G protein-coupled receptors. Gene 387:38–48.

Blanpain C, Fuchs E. 2006. Epidermal stem cells of the skin. Annu Rev Cell Dev Biol 22:339–373.

Cash JL, Hart R, Russ A, Dixon JP, Colledge WH, Doran J, Hendrick AG, Carlton MB, Greaves DR. 2008. Synthetic chemerin-derived peptides suppress inflammation through ChemR23. J Exp Med 205:767–775.

Chang GW, Stacey M, Kwakkenbos MJ, Hamann J, Gordon S, Lin HH. 2003. Proteolytic cleavage of the EMR2 receptor requires both the extracellular stalk and the GPS motif. FEBS Lett 547: 145–150.

Davies B, Baumann C, Kirchhoff C, Ivell R, Nubbemeyer R, Habenicht UF, Theuring F, Gottwald U. 2004. Targeted deletion of the epididymal receptor HE6 results in fluid dysregulation and male infertility. Mol Cell Biol 24: 8642–8648.

Fredriksson R, Lagerstrom MC, Hoglund PJ, Schioth HB. 2002. Novel human G protein-coupled receptors with long N-terminals containing GPS domains and Ser/Thr-rich regions. FEBS Lett 531: 407–414.

Fredriksson R, Lagerström MC, Lundin L-G, Schiöth HB. 2003. The G-protein-coupled receptors in the human genome form five main families. Phylogenetic analysis, paralogon groups, and fingerprints. Mol Pharmacol 63: 1256–1272.

Fukuzawa T, Hirose S. 2006. Multiple processing of Ig-Hepta/GPR116, a G protein-coupled receptor with immunoglobulin (Ig)-like repeats, and generation of EGF2-like fragment. J Biochem (Tokyo) 140:445–452.

Haitina T, Olsson F, Stephansson O, Alsio J, Roman E, Ebendal T, Schioth HB, Fredriksson R. 2008. Expression profile of the entire family of Adhesion G

protein-coupled receptors in mouse and rat. BMC Neurosci 9:43.
Hardman MJ, Sisi P, Banbury DN, Byrne C. 1998. Patterned acquisition of skin barrier function during development. Development 125:1541–1552.
Higgins DG, Bleasby AJ, Fuchs R. 1992. CLUSTAL V: improved software for multiple sequence alignment. Comput Appl Biosci 8:189–191.
Krasnoperov VG, Bittner MA, Beavis R, Kuang Y, Salnikow KV, Chepurny OG, Little AR, Plotnikov AN, Wu D, Holz RW, Petrenko AG. 1997. alpha-Latrotoxin stimulates exocytosis by the interaction with a neuronal G-protein-coupled receptor. Neuron 18:925–937.
Laemmli UK. 1970. Cleavage of structural proteins during the assembly of the head of bacteriophage T4. Nature 227:680–685.
Langenhan T, Prömel S, Mestek L, Esmaeili B, Waller-Evans H, Hennig C, Kohara Y, Avery L, Vakonakis I, Schnabel R, Russ AP. 2009. Latrophilin signaling links anterior-posterior tissue polarity and oriented cell divisions in the C. elegans embryo. Dev Cell 17: 494–504.
Lim A, Zhang L. 1999. WebPHYLIP: a web interface to PHYLIP. Bioinformatics 15:1068–1069.
Lin HH, Chang GW, Davies JQ, Stacey M, Harris J, Gordon S. 2004. Autocatalytic cleavage of the EMR2 receptor occurs at a conserved G protein-coupled receptor proteolytic site motif. J Biol Chem 279:31823–31832.
Lin HH, Faunce DE, Stacey M, Terajewicz A, Nakamura T, Zhang-Hoover J, Kerley M, Mucenski ML, Gordon S, Stein-Streilein J. 2005. The macrophage F4/80 receptor is required for the induction of antigen-specific efferent regulatory T cells in peripheral tolerance. J Exp Med 201:1615–1625.
Lum AM, Wang BB, Beck-Engeser GB, Li L, Channa N, Wabl M. 2010. Orphan receptor GPR110, an oncogene overexpressed in lung and prostate cancer. BMC Cancer 10:40.
Monk KR, Naylor SG, Glenn TD, Mercurio S, Perlin JR, Dominguez C, Moens CB, Talbot WS. 2009. A G protein-coupled receptor is essential for Schwann cells to initiate myelination. Science 325:1402–1405.
Monk KR, Oshima K, Jors S, Heller S, Talbot WS. 2011. Gpr126 is essential for peripheral nerve development and myelination in mammals. Development 138:2673–2680.
Nordstrom KJ, Lagerstrom MC, Waller LM, Fredriksson R, Schioth HB. 2009. The Secretin GPCR descended from the family of Adhesion GPCR. Mol Biol Evol 26:71–84.
Prömel S, Frickenhaus M, Hughes S, Mestek L, Staunton D, Woollard A, Vakonakis I, Schöneberg T, Schnabel R, Russ A, Langenhan T. 2012. The GPS motif is a molecular switch for bimodal activities of adhesion-class G protein-coupled receptors. Cell Rep (In press).
Russ AP, Wattler S, Colledge WH, Aparicio SA, Carlton MB, Pearce JJ, Barton SC, Surani MA, Ryan K, Nehls MC, Wilson V, Evans MJ. 2000. Eomesodermin is required for mouse trophoblast development and mesoderm formation. Nature 404:95–99.
Silva JP, Lelianova V, Hopkins C, Volynski KE, Ushkaryov Y. 2009. Functional cross-interaction of the fragments produced by the cleavage of distinct adhesion G-protein-coupled receptors. J Biol Chem 284:6495–6506.
Steinert M, Wobus M, Boltze C, Schutz A, Wahlbuhl M, Hamann J, Aust G. 2002. Expression and regulation of CD97 in colorectal carcinoma cell lines and tumor tissues. Am J Pathol 161:1657–1667.
Thompson JD, Higgins DG, Gibson TJ. 1994. CLUSTAL W: improving the sensitivity of progressive multiple sequence alignment through sequence weighting, position-specific gap penalties and weight matrix choice. Nucleic Acids Res 22:4673–4680.
Usui T, Shima Y, Shimada Y, Hirano S, Burgess RW, Schwarz TL, Takeichi M, Uemura T. 1999. Flamingo, a seven-pass transmembrane cadherin, regulates planar cell polarity under the control of Frizzled. Cell 98:585–595.
Vakonakis I, Langenhan T, Prömel S, Russ A, Campbell ID. 2008. Solution structure and sugar-binding mechanism of mouse latrophilin-1 RBL: a 7TM receptor-attached lectin-like domain. Structure 16:944–953.
Waller-Evans H, Prömel S, Langenhan T, Dixon J, Zahn D, Colledge WH, Doran J, Carlton MB, Davies B, Aparicio SA, Grosse J, Russ AP. 2010. The orphan adhesion-GPCR GPR126 is required for embryonic development in the mouse. PLoS One 5:e14047.
Wessel D, Flugge UI. 1984. A method for the quantitative recovery of protein in dilute solution in the presence of detergents and lipids. Anal Biochem 138:141–143.
Wu C, Orozco C, Boyer J, Leglise M, Goodale J, Batalov S, Hodge CL, Haase J, Janes J, Huss JWIII, Su AI. 2009. BioGPS: an extensible and customizable portal for querying and organizing gene annotation resources. Genome Biol 10:R130.